ON THE CAPACITY OF ORIENTATION MODULATION HALFTONE CHANNELS

Orhan Bulan, Gaurav Sharma

University of Rochester, ECE Dept.,
Rochester, NY, 14627-0126, USA

Vishal Monga

Xerox Research Center Webster
Webster, NY, 14580, USA

ABSTRACT

Clustered-dot halftones are extensively utilized in hardcopy printing. Modulation of the dot orientation in these halftones offers an avenue for data embedding which has been exploited in a number of different methods. We consider the capacity of these channels, modeling them as binary orientation input channels with vector valued output detection statistics. We derive upper bounds on the capacity for three channel conditional distributions corresponding to sub-Gaussian, Gaussian and super-Gaussian distributions. Using experimentally estimated channel parameters our bounds reveal that channel capacity has noticeable variations as a function of gray level. Highlights, shadows and mid-tones offer negligible capacity, on the contrary the regions between highlights and mid-tones or shadows and mid-tones offer high capacity for data embedding.

Index Terms— Orientation modulation halftone channel, capacity, print watermark

1. INTRODUCTION

Digital halftoning is extensively employed for the purpose of reducing an original continuous tone (typically 8 bits/pixel) image to a 1 bit/pixel binary image that is suitable for printing on binary output devices such as lithographic printing presses, laser and inkjet printers, etc. For a variety of applications, the capability to imperceptibly embed data in printed documents is desirable(see, for example [1]). Accordingly, a number of methods have been proposed for embedding data in printed halftone images[2, 3, 4, 5, 6, 7, 8, 9]. A significant class of techniques is the set of methods that utilizes the orientation of clustered halftone dots for the purpose of embedding [5, 10, 11]. These methods utilize elliptic shaped clustered halftone dots whose orientation is varied in order to embed information in the printed document.

The process of embedding in orientation is well suited to halftone print-processes. The halftoning relies on the fact that the viewer perceives a spatial average of the halftones and alterations of the dot orientation do not change the average gray level. Orientation based embedding therefore introduces low visual distortion. For orientation based embedding, at the decoder, the encoded orientation must be identified from a scan of the printed image. This typically involves the use of statistical criteria[10, 11] employed in conjunction with a probabilistic model of print-scan channel. A characterization of the apposite print-scan channel is therefore desirable: both in order to adapt the embedding to the characteristics of the print-scan distortion channel and to quantify the limits of embedding. The former is also desirable from the now well-known analogy between robust data hiding and communications with side information [12].

This paper provides capacity upper bounds for orientation modulation halftone channels. Our work reveals that the channel capacity shows considerable variation as a function of the gray level. This result helps in identifying hiding friendly gray levels.

2. ORIENTATION MODULATION HALFTONE CHANNELS

In the case of data embedding by halftone orientation modulation in clustered dot halftones, the inherent periodic structure of the halftones provides a mechanism for synchronization. In particular, the periodicity of the halftone grid can be readily estimated from a scan of the printed image (for example, by computing a Fourier transform and finding the peaks corresponding to the principal frequency). Once this periodicity is recovered, the synchronization can be inferred [11, 13]. We therefore consider the problem of capacity under the assumption of synchronization. Furthermore, in order to simplify our analysis, we analyze the capacity for a single gray level and examine the variation in capacity as the gray level is varied.

For the purpose of estimating their capacity, orientation modulation channels can be represented by the model shown in Fig. 1. In this model, the channel input is the orientation Θ for the halftone dot and the output are the (vector-valued) detection statistics $\underline{\Sigma}$ obtained from the printed and scanned version of the dot. These statistics may correspond, for instance, to binary correlations in the case of DataGlyphs [14], or to image moments estimated from the scans [11]. In practical printing systems, the process of printing inherently introduces a directional asymmetry, which when coupled with

This work was supported in part by Xerox Foundation and by a grant from New York State Office of Science, Technology and Academic Research (NYSTAR) through the Center for Electronic Imaging Systems (CEIS).

arbitrary orientation modulation results in an unintended and undesirable variation in the average gray level of the printed halftone. Thus in order to limit perceptible distortion practical data embedding systems based on orientation modulation limit the orientations of the dots to two orthogonally oriented directions with respect to which the printing process is symmetric, for example $\pm 45\,\mathrm{deg}$ with respect to the direction of paper feed. This symmetry ensures that the orientation modulation causes no change in average gray level of the printed halftone - thus eliminating (or at least very significantly reducing) potential embedding artifacts. Accordingly for the purpose of estimating capacity, we assume that the input Θ is binary.

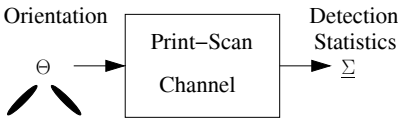

Fig. 1. Orientation modulation channel model.

For our model of the orientation modulation halftone channel, the expression for capacity can be written as

$$\begin{aligned} C &= \max_{p(\theta)} I(\Theta;\underline{\Sigma}) \\ &= \max_{p(\theta)} \Big[h(\underline{\Sigma}) - h(\underline{\Sigma}|\Theta)\Big] \end{aligned} \tag{1}$$

where $h(\underline{\Sigma})$ denotes the differential entropy of the random vector $\underline{\Sigma}$ representing the detection statistics, and $h(\underline{\Sigma}|\Theta)$ denotes the conditional differential entropy of $\underline{\Sigma}$ given the orientation $\underline{\Theta}$.

3. CAPACITY BOUNDS FOR ORIENTATION MODULATION CHANNELS

In this section, we give upper bounds for the capacity of the orientation modulation channel for various channel distributions. We bound the channel capacity by finding an upper bound for the joint entropy of detection statistics $h(\underline{\Sigma})$ and evaluating the conditional entropy $h(\underline{\Sigma}|\Theta)$ in (1). [1]

Noting that Θ is binary we can write $h(\underline{\Sigma}|\Theta) = \sum_{i=1}^{2} p(\theta_i)$ $h(\underline{\Sigma}|\Theta = \theta_i)$ which substituted in the capacity expression of (1), yields

$$C = \max_{p(\theta)} \Big[h(\underline{\Sigma}) - \sum_{i=1}^{2} p(\theta_i) h(\underline{\Sigma}|\Theta = \theta_i)\Big] \tag{2}$$

where Θ represents the binary orientation and $\underline{\Sigma}$ is a $n \times 1$ vector that holds detection statistics along different orientations. Let $K_{\underline{\Sigma}}$ denote the $n \times n$ covariance matrix of the detection statistics $\underline{\Sigma}$. Observing that among all n-dimensional distributions with covariance $K_{\underline{\Sigma}}$, the Gaussian distribution has the maximum differential entropy [15], we see that

$$h(\underline{\Sigma}) \leq [\frac{1}{2} \ln\big[(2\pi e)^n \det(K_{\underline{\Sigma}})\big] \tag{3}$$

where the right hand side is obtained from the expression for the differential entropy of a multivariate gaussian with covariance $K_{\underline{\Sigma}}$. Using (3) in (2), we obtain an upper bound on the capacity as

$$C \leq \max_{p(\theta)} \Big[\frac{1}{2} \ln\big[(2\pi e)^n \det(K_{\underline{\Sigma}})\big] - \sum_{i=1}^{2} p(\theta_i) h(\underline{\Sigma}|\Theta = \theta_i)\Big] \tag{4}$$

3.1. Channel Model

Though the channel model shown in the Fig. 1 is valid for orientation modulation channels with any detection statistics, we specifically focus on moment based detection in this paper.

Evaluation of the multi-dimensional conditional entropy $h(\underline{\Sigma}|\Theta)$ is a hard task especially when the corresponding multi-dimensional density function is not available. Here, the detection statistics vector $\underline{\Sigma}$ comprises of moments σ_x and σ_y evaluated along the two orthogonal directions corresponding to the input modulation [11]. For the two orientation case, assuming conditional independence, the joint density function of output statistics becomes:

$$f_{\underline{\Sigma}|\Theta}(\underline{\sigma}|\theta) = f_{\Sigma_x|\Theta}(\sigma_x|\theta) f_{\Sigma_y|\Theta}(\sigma_y|\theta) \tag{5}$$

Corresponding joint entropy is hence expressed as:

$$h(\underline{\Sigma}|\Theta) = h(\Sigma_x|\Theta) + h(\Sigma_y|\Theta) \tag{6}$$

Figure 2 illustrates the simplified probabilistic model of the orientation channel.

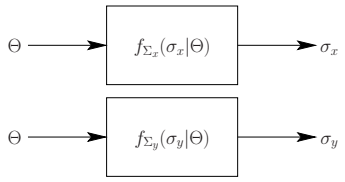

Fig. 2. Simplified probabilistic model for the channel.

In previous work [11], we validated this assumption of conditional independence[2](separable) by empirically obtaining estimates of 2×2 covariance matrices for different gray levels. It follows that the upper bound for the capacity becomes

$$\begin{aligned} C \leq \max_{p(\theta)} \Big[\frac{1}{2} \ln\big[(2\pi e)^2 \det(K_{\underline{\Sigma}})\big] \\ - \sum_{i=1}^{2} p(\theta_i) \big[h(\Sigma_x|\Theta = \theta_i) + h(\Sigma_y|\Theta = \theta_i)\big]\Big] \end{aligned} \tag{7}$$

[1] This is readily generalizable to the general M-ary case.

[2] Strictly, conditional uncorrelatedness.

Evaluating the conditional entropy $h(\Sigma_x|\Theta=\theta_i)$, $h(\Sigma_y|\Theta=\theta_i)$ requires a characterization of conditional densities $f_{\Sigma_x|\Theta}(\sigma_x|\theta)$ and $f_{\Sigma_y|\Theta}(\sigma_y|\theta)$. The symmetry described earlier for the embedding process and the print-scan channel motivates the following symmetry constraints on their conditional densities.

$$f_{\Sigma_x|\Theta}(t|0) = f_{\Sigma_y|\Theta}(t|1) \quad ,\forall t \tag{8}$$
$$f_{\Sigma_x|\Theta}(t|1) = f_{\Sigma_y|\Theta}(t|0) \quad ,\forall t \tag{9}$$

Additionally, we observe that these conditional densities vary depending on the gray level. In order to accommodate this variability and the variation over different printers, we model the channel conditional densities using three distinct parametrized families belonging to sub-gaussian ($\gamma < 3$), gaussian ($\gamma = 3$) and super-gaussian ($\gamma > 3$) categories where γ denotes the widely accepted shape descriptor, i.e., the kurtosis [16].

3.1.1. Laplacian Channel (Super-Gaussian)

The probability density function of Laplacian distribution is defined as $f_X(x) = \frac{1}{2\lambda} exp(-\frac{|x-\mu|}{\lambda})$. The differential entropy is computed as

$$\begin{aligned} h(X) &= -\int_{-\infty}^{\infty} f_X(x)\ln(f_X(x))dx \\ &= \int_{-\infty}^{\infty} \ln(2\lambda) f_X(x)dx + \int_{-\infty}^{\infty} \frac{|x-\mu|}{\lambda} f_X(x)dx \\ &= \ln(2\lambda)+1 \end{aligned} \tag{10}$$

Then, each conditional entropy in (7) is replaced with the exact entropy expression for the laplacian channel and the upper bound for the capacity is given by

$$C \le \max_{p(\theta)} \Big[\frac{1}{2}\ln\big[(2\pi e)^2 \det(K_{\underline{\Sigma}})\big] - \sum_{i=1}^{2} p(\theta_i)\big[\ln(2e\lambda_{x_i}) + \ln(2e\lambda_{y_i})\big]\Big] \tag{11}$$

λ_{x_i} and λ_{y_i} are parameters of (marginal) conditional density functions of moments where conditioning is performed on two orthogonal horizontal and vertical orientations.

3.1.2. Gaussian Channel

The probability density function for Gaussian channel is $f_X(x) = \frac{1}{s\sqrt{2\pi}} \exp\big(-\frac{(x-\mu)^2}{2s^2}\big)$ where s denotes the standard deviation of the distribution. Differential entropy for a Gaussian is well-known [15] and given by $h(X) = \ln(s\sqrt{2\pi e})$. Substituting the conditional entropies in (7), the upper bound for the capacity is found as:

$$C \le \max_{p(\theta)} \Big[\frac{1}{2}\ln\big[(2\pi e)^2 \det(K_{\underline{\Sigma}})\big] - \sum_{i=1}^{2} p(\theta_i) \big[\ln(s_{x_i}\sqrt{2\pi e}) + \ln(s_{y_i}\sqrt{2\pi e})\big]\Big] \tag{12}$$

s_{x_i} and s_{y_i} $i = 1, 2$ are standard deviations of conditional densities of moments.

3.1.3. Triangular Channel (Sub-Gaussian)

The probability density function of triangular distribution is defined as:

$$f_X(x) = \begin{cases} \frac{2(x-a)}{(b-a)(c-a)} & \text{for } a \le x \le c \\ \frac{2(b-x)}{(b-a)(b-c)} & \text{for } c \le x \le b \end{cases}$$

The differential entropy is calculated as

$$h(X) = -\int_a^c f_X(x)\ln[f_X(x)]dx - \int_c^b f_X(x)\ln[f_X(x)]dx$$

The first integral is computed as

$$\begin{aligned} h(X) &= \int_a^c \ln[(b-a)(c-a)] f_X(x)dx \\ &\quad - \int_a^c f_X(x)\ln(2(x-a))dx \\ &= \frac{(c-a)}{(b-a)}\ln[(b-a)(c-a)] - \frac{1}{(b-a)(c-a)} \\ &\quad \int_a^c 2(x-a)\ln[2(x-a)]dx \\ &= \frac{(c-a)}{(b-a)}\Big(\ln\big[\frac{(b-a)}{2}\big] + \frac{1}{2}\Big) \end{aligned} \tag{13}$$

Second integral may be evaluated similarly and the differential entropy for the triangular distribution becomes

$$h(X) = \frac{1}{2} + \ln(\frac{b-a}{2}) \tag{14}$$

Hence, the upper bound for the channel capacity is given by:

$$C \le \max_{p(\theta)} \Big[\frac{1}{2}\ln\big[(2\pi e)^2 \det(K_{\underline{\Sigma}})\big] - \sum_{i=1}^{2} p(\theta_i) \big[\frac{1}{2} + \ln(\frac{b_{x_i}-a_{x_i}}{2}) + \frac{1}{2} + \ln(\frac{b_{y_i}-a_{y_i}}{2})\big]\Big] \tag{15}$$

Note that in the expressions for the capacity upper bounds in the preceding subsections, $K_{\underline{\Sigma}}$ depends on $p(\theta)$. In each of the cases, it can be shown that an equiprobable distribution for $p(\theta)$ achieves the maxima that defines the capacity upper bounds.

4. CAPACITY FOR DIFFERENT GRAY LEVELS

We perform an experiment to identify the gray levels that offer high capacity and are therefore appropriate for embedding. For this purpose, channel parameters need to be estimated experimentally for each gray level.

We utilized a 2400 dpi xerographic printer and generate 8 inch by 8 inch constant gray level images with halftone screen frequency of 75 lines per inch. From the scans of the printed image we compute moments in the ± 45 deg directions for each of the embedding orientations. We estimate the parameters of various conditional densities in Sections 3.1.1- 3.1.3 via expectation maximization [17].

Plots of channel capacity bounds as a function of gray level are shown in Fig. 3. For simplicity, we plot capacity assuming Gaussian and Laplacian channels for all gray levels. As evident from the plot, the capacity is negligibly small in the mid-tones $(100 - 130)$, highlights(< 40) and shadows(> 180). The region between highlights and mid-tones, and mid-tones and highlights offers considerably higher capacity. The "double hump" shape for the capacity follows intuition as the number of available halftone configurations is severely restricted in highlights, shadows and mid-tones. In the extreme case of purely black or white regions, only a single halftone configuration is possible and hence the capacity is zero. Likewise, at mid-tones the number of available halftone configurations is very small. The mismatch in the heights of the two peaks is attributed to the asymmetric dot gain that occurs in the physical printing process and is more pronounced in darker as opposed to lighter regions.

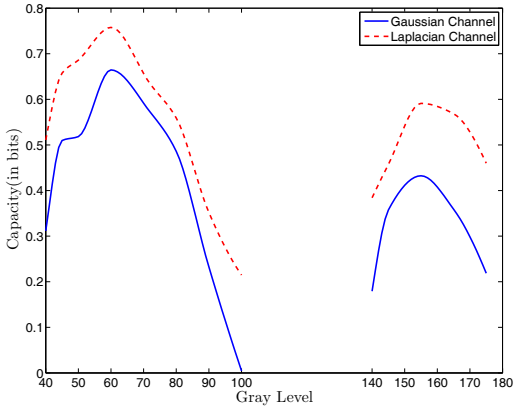

Fig. 3. Capacity bounds for the orientation modulation channel with Gaussian and Laplacian channel conditional distributions. Gray level range is from 0 to 255. Gray level 0 corresponds to white and gray level 255 corresponds to black.

5. CONCLUSION

We investigate the capacity of orientation modulation channels for data embedding in printed halftones. We obtain upper bounds for the capacity of these channels as a function of the average gray level. To account for varying channel characteristics encountered in practice, we select examples from each of the super-Gaussian, Gaussian and sub-Gaussian distribution categories and compute capacity bounds in each case. Evaluations of the capacity bounds using empirically estimated channel parameters from actual prints, reveal that highlights, shadows and mid-tones offer small capacity, but in regions from white to mid-tone and mid-tone to black high capacity is available. Although we specifically focus on moment based detection scenario in this paper, similar capacity bounds are applicable to other orientation modulation channels e.g. with correlation based detection.

.

6. REFERENCES

[1] DigiMarc Corp, "Digimarc mediabridge," 2000.

[2] K. Tanaka, Y. Nakamura, and K. Matsui, "Embedding secret information into a dithered multi-level image," *Proc. IEEE Military Communications Conf.*, pp. 216–220, Sept. 1990.

[3] Z. Baharav and D. Shaked, "Watermarking of dithered halftone images," vol. 3657, pp. 307–316, Jan. 1999.

[4] D. Kacker and J. P. Allebach, "Joint halftoning and watermarking," *IEEE Trans. Sig. Proc.*, , no. 4, pp. 243 – 257, Apr. 2003.

[5] C. Liu, S. Wang, and B. Xu, "Authenticate your digital prints with Glossmark images," in *Proceedings IS&T NIP20: International Conference on Digital Printing Technologies*, Oct. 2004, pp. 312–316.

[6] N. Damera-Venkata, J. Yen, V. Monga, and B. L. Evans, "Hardcopy image barcodes via block error diffusion," *IEEE Trans. Image Proc.*, vol. 14, no. 12, pp. 1977–1989, 2005.

[7] K. T. Knox and S.-G. Wang, "Digital watermarks using stochastic screens," in *Proc. SPIE: Color Imaging: Device Independent Color, Color Hardcopy, and Graphic Arts II*, G. B. Beretta and R. Eschbach, Eds., Feb. 1997, vol. 3018, pp. 316–322.

[8] G. Sharma and S.-G. Wang, "Show-through watermarking of duplex printed documents," in *Proc. SPIE: Security, Steganography, and Watermarking of Multimedia Contents VI*, E. J. Delp and P. W. Wong, Eds., Jan. 2004, vol. 5306.

[9] B. Oztan and G. Sharma, "Continuous phase modulated halftones and their application to halftone data embedding," in *Proc. IEEE Intl. Conf. Acoustics Speech and Sig. Proc.*, May 2006, vol. II, pp. 333–336.

[10] D. L. Hecht, "Printed embedded data graphical user interfaces," *IEEE Computer*, pp. 47–55, Mar. 2001.

[11] O. Bulan, V. Monga, G. Sharma, and B. Oztan, "Data embedding in hardcopy images via halftone dot-orientation modulation," in Security, Forensics, Steganography, and Watermarking of Multimedia Contents X, Electronic Imaging Symp. 27-31 Jan. 2008, San Jose, CA, accepted for presentation.

[12] I. J. Cox, M. L. Miller, and J. A. Bloom, *Digital Watermarking*, Morgan Kaufmann, 2001.

[13] K. Solanki, U. Madhow, B. S. Manjunath, S. Chandrasekaran, and I. El-Khalil, "Print and scan resilient data hiding in images," *IEEE Trans. Info. Forensics and Security*, vol. 1, no. 4, pp. 464–478, Dec. 2006.

[14] D. L. Hecht, "Embedded data glyph technology for hardcopy digital documents," in *Proc. SPIE: Color hard copy and graphic arts III*, J. Bares, Ed., Feb. 1994, vol. 2171, pp. 341–352.

[15] C. E. Shannon, "A mathematical theory of communication," *Bell Sys. Tech. J.*, vol. 27, pp. 379–423, 623–656, 1948.

[16] Kaddour Najim, Enso Ikonen, and Ait-Kadi Daoud, *Stochastic Processes:Estimation, Optimisation and Analysis*, Sterling, VA : Kogan Page Science, London, UK, 2004.

[17] J. Salojarvi and K. Puolamaki, "Expectation maximization algorithms for conditional likelihoods," *Proc. 22nd International Conference on Machine Learning*, Aug. 2005.